

# Viscosities, diffusion coefficients, and mixing times of intrinsic fluorescent organic molecules in brown limonene secondary organic aerosol and tests of the Stokes-Einstein equation

5 Dagny A. Ullmann<sup>1</sup>, Mallory L. Hinks<sup>2</sup>, Adrian Maclean<sup>1</sup>, Christopher Butenhoff<sup>3</sup>, James Grayson<sup>1</sup>, Kelley Barsanti<sup>5</sup>, Jose L. Jimenez<sup>4</sup>, Sergey A. Nizkorodov<sup>2</sup>, Saeid Kamal<sup>1</sup>, Allan K. Bertram<sup>1</sup>

<sup>1</sup>Department of Chemistry, University of British Columbia, Vancouver, BC, V6T 1Z1, Canada

<sup>2</sup>Department of Chemistry, University of California, Irvine, CA 92697, USA

<sup>3</sup>Department of Physics, Portland State University, Portland, Oregon, USA

10 <sup>4</sup>Cooperative Institute for Research in the Environmental Sciences and Department of Chemistry and Biochemistry, University of Colorado, Boulder, CO, USA

<sup>5</sup>Department of Chemical and Environmental Engineering and Center for Environmental Research and Technology, University of California, Riverside, CA, USA

15 *Correspondence to:* Allan K. Bertram ([bertram@chem.ubc.ca](mailto:bertram@chem.ubc.ca)) and Saeid Kamal ([skamal@chem.ubc.ca](mailto:skamal@chem.ubc.ca))

## Abstract.

Viscosities and diffusion rates of organics within secondary organic aerosol (SOA) remain uncertain. Using the bead-mobility  
20 technique, we measured the viscosities as a function of water activity ( $a_w$ ) of SOA generated by the ozonolysis of limonene followed by browning by exposure to  $\text{NH}_3$  (referred to as brown limonene SOA or brown LSOA). These measurements together with viscosity measurements reported in the literature show that the viscosity of brown LSOA increases by 3-5 orders of magnitude as the  $a_w$  decreases from 0.9 to approximately 0.05. In addition, we measured diffusion coefficients of intrinsic fluorescent organic molecules within brown LSOA matrices using rectangular area fluorescence recovery after photobleaching.  
25 Based on the diffusion measurements, as the  $a_w$  decreases from 0.9 to 0.33, the average diffusion coefficient of the intrinsic fluorescent organic molecules decreases from  $5.5 \cdot 10^{-9} \text{ cm}^2 \text{ s}^{-1}$  to  $7.1 \cdot 10^{-13} \text{ cm}^2 \text{ s}^{-1}$  and the mixing times of intrinsic fluorescent organic molecules within 200 nm brown LSOA particles increases from 0.002 s to 14 s. These results suggest that the mixing times of large organics in the brown LSOA studied here are short ( $< 1 \text{ hr}$ ) for  $a_w$  and temperatures often found in the planetary boundary layer. Since the diffusion coefficients and mixing times reported here correspond to SOA generated using a high  
30 mass loading ( $\sim 1,000 \mu\text{g m}^{-3}$ ), biogenic SOA particles found in the atmosphere with mass loadings  $\leq 10 \mu\text{g m}^{-3}$  are likely to have higher viscosities and longer mixing times (possibly 3 orders of magnitude longer). These new measurements of viscosity and diffusion were used to test the accuracy of the Stokes-Einstein relation for predicting diffusion rates of organics within brown LSOA matrices. The results show that the Stokes-Einstein equation gives accurate predictions of diffusion coefficients of large organics within brown LSOA matrices when the viscosity of the matrix is as high as  $10^2$  to  $10^4 \text{ Pa s}$ . These results  
35 have important implications for predicting diffusion and mixing with SOA particles in the atmosphere.

## 1 Introduction

40 Large amounts of volatile organic compounds, such as isoprene, limonene, and  $\alpha$ -pinene from biogenic sources and aliphatic and aromatic compounds from anthropogenic sources are released into the atmosphere. These compounds can be oxidized by a complex series of atmospheric reactions to form lower-volatility products that condense to form secondary organic aerosols (SOA) (Hallquist et al., 2009;Kanakidou et al., 2005). SOA makes up approximately 30-70% of the mass of atmospheric particles (Kanakidou et al., 2005;Jimenez et al., 2009). Due to the hygroscopic nature of SOA, an important component of  
45 SOA particles is water (Bateman et al., 2015;Hildebrandt Ruiz et al., 2015;Massoli et al., 2010). The amount of water in SOA particles is determined by the relative humidity (RH); as the RH increases, the water activity ( $a_w$ ) (and hence water content) in SOA particles increases to maintain equilibrium with the gas phase. SOA particles can influence climate either directly by absorbing or scattering sunlight or indirectly by acting as cloud condensation nuclei (CCN) or ice nuclei (IN) (Kanakidou et al., 2005;Murray et al., 2010;Solomon, 2007;Wang et al., 2012). SOA particles can also influence air quality and public health  
50 (Baltensperger et al., 2008;Jang et al., 2006;Poschl and Shiraiwa, 2015;Shiraiwa et al., 2017b).

Despite the importance of SOA particles in climate and air quality, their physicochemical properties remain poorly understood (Hallquist et al., 2009). This leads to uncertainties when predicting the role of SOA particles in atmospheric chemistry, climate, and air quality (Hallquist et al., 2009;Shiraiwa and Seinfeld, 2012;Shrivastava et al., 2017a;Zaveri et al., 2014). One  
55 physicochemical property that remains poorly known is the rate of diffusion of organics within SOA particles (Liu et al., 2016;Shiraiwa et al., 2013;Shrivastava et al., 2017a;Ye et al., 2016). Information on diffusion rates is needed to predict the reactivity and photochemistry of SOA particles (Chu and Chan, 2017;Davies and Wilson, 2015;Gržinić et al., 2015;Houle et al., 2015;Li et al., 2015;Lignell et al., 2014;Shiraiwa et al., 2011;Wang et al., 2015). Diffusion rates are also needed to predict the growth rates, size distributions, cloud condensation ability, and ice nucleating ability of SOA particles (Boyd et al.,  
60 2017;Huff Hartz et al., 2005;Murray et al., 2010;Perraud et al., 2012;Riipinen et al., 2011;Shiraiwa and Seinfeld, 2012;Solomon and (eds.), 2007;Taina et al., 2017;Wagner et al., 2017;Wang et al., 2012;Zaveri et al., 2014;Zaveri et al., 2018). Slow diffusion of molecules in particles also has implications for the long-range transport of pollutants (Bastelberger et al., 2017;Shrivastava et al., 2017b;Zelenyuk et al., 2012;Zhou et al., 2012) and the optical properties of particles (Adler et al., 2013;Robinson et al., 2014).

65

To estimate diffusion rates of organics in SOA particles, it is common to use viscosity measurements together with the Stokes-Einstein relation (Booth et al., 2014;Hosny et al., 2013;Koop et al., 2000;Power et al., 2013;Renbaum-Wolff et al., 2013a;Shiraiwa et al., 2011;Shiraiwa et al., 2017a;Song et al., 2015;Song et al., 2016),

$$D = \frac{kT}{6\pi\eta R_H} \quad (1)$$

70 where  $D$  is the diffusion coefficient of the diffusing species,  $k$  is the Boltzmann constant,  $T$  is the temperature,  $\eta$  is the dynamic  
viscosity and  $R_H$  is the hydrodynamic radius of the diffusing species. Until now, the accuracy of the Stokes-Einstein relation  
for predicting diffusion rates of organics in SOA particles has not been quantified, leading to uncertainties when estimating  
diffusion rates from viscosity measurements. Motivated primarily by the food industry, there have been a few tests of the  
Stokes-Einstein relation for predicting diffusion rates of organics in organic-water matrices, such as saccharide-water matrices  
75 (Bastelberger et al., 2017;Champion et al., 1997;Chenyakin et al., 2017;Corti et al., 2008;Price et al., 2016). In these cases, the  
matrices contained only two species (one organic and water), which is very different from SOA matrices that contain thousands  
of different species (Nozière et al., 2015).

In the future, researchers will likely continue to use viscosity data combined with the Stokes-Einstein relation to estimate  
80 diffusion rates of organics in SOA particles, because several techniques have been developed recently to measure the  
viscosities of SOA matrices and proxies of SOA matrices (Bateman et al., 2015;Grayson et al., 2016b;Lee et al., 2017;Marsh  
et al., 2017;Price et al., 2015;Reid et al., 2018;Renbaum-Wolff et al., 2013a;Song et al., 2015;Zhang et al., 2015). As a result,  
the accuracy of the Stokes-Einstein relation for predicting diffusion rates of organics in SOA particles needs to be quantified.

85 In the following, we measured the viscosities of brown limonene SOA (brown LSOA) as a function of  $a_w$  using the bead-  
mobility technique. The brown LSOA is a product of exposure of white limonene ozonolysis SOA to ppb levels of ammonia  
vapour (Laskin et al., 2010), and it is a model system for the formation of secondary brown carbon (Laskin et al., 2015). In  
addition, we measured diffusion coefficients of intrinsic fluorescent organic molecules within brown LSOA matrices using a  
technique called rectangular area fluorescence recovery after photobleaching. These new data, combined with viscosity data  
90 that already exist in the literature for brown LSOA-water matrices, were used to test the accuracy of the Stokes-Einstein relation  
for predicting diffusion rates of organics within SOA particles. We also used the measured diffusion coefficients to estimate  
mixing times of organics within 200 nm brown LSOA particles at RHs typically found in the planetary boundary layer (the  
region of the atmosphere from the surface to an altitude of up to 1 km). We focused on brown LSOA for the following reasons:  
first, brown LSOA contains light absorbing molecules that are also fluorescent (here referred to as intrinsic fluorescent organic  
95 molecules) and capable of rapid photobleaching (Lee et al., 2013). These intrinsic fluorescent organic molecules offer a key  
advantage because one can measure diffusion coefficients within brown LSOA using rectangular area fluorescence recovery  
after photobleaching without the need to add a foreign tracer fluorescent molecule to the SOA matrix. Second, limonene  
accounts for roughly 10 % of the global emissions of monoterpenes (and is thus an important source of SOA in the atmosphere)  
(Kanakidou et al., 2005;Sindelarova et al., 2014).

## 100 2 Experimental

### 2.1 Generation of brown LSOA

Brown LSOA was produced at the University of California-Irvine (UCI) following the procedure outlined in Hinks et al. (2016). First, particles consisting of limonene secondary organic material (LSOA) were generated in a 20 L flow tube by dark ozonolysis of d-limonene. Mixing ratios of ozone and d-limonene (97% Sigma-Aldrich) were both 10 ppm prior to  
105 reaction. Ozone was produced externally to the flow tube by an electric discharge in pure O<sub>2</sub> (Ultra High Purity, Airgas). After the ozonolysis reaction, the mass concentration of LSOA particles within the flow tube was approximately 1,000 µg/m<sup>3</sup>. At the exit of the flow tube, the carrier gas and LSOA particles were passed through a charcoal denuder to eliminate excess ozone and gas-phase organics, followed by collection of the LSOA particles on hydrophobic slides (Hampton Research; Aliso Viejo, CA, USA) using a Sioutas impactor with a single stage “D” (0.25 µm cut point at 9 SLM collection flow rate). After LSOA  
110 production, the hydrophobic slides containing the LSOA were placed within a small glass petri dish, which was left floating on the surface of a solution of 0.1 M ammonium sulfate (>99 %, EMD) in a larger, covered petri dish. Over a period of three to five days, the ammonia vapour in equilibrium with the ammonium sulfate solution (concentration estimated to be 300 ppb NH<sub>3</sub> using the Extended AIM Aerosol Thermodynamics Model II) (Clegg et al., 1998) reacted with the fresh LSOA forming a visible brown colour. After production of the brown LSOA, the samples were shipped to the University of British Columbia  
115 for viscosity and diffusion coefficient measurements.

### 2.2 Viscosity measurements

The viscosities of brown LSOA particles were determined at  $a_w$  of approximately 0.7, 0.8 and 0.9, using the bead mobility technique (Renbaum-Wolff et al., 2013b). At lower  $a_w$ , the viscosities were too high for measurements with this technique. In  
120 short, small particles (5-50 µm in diameter) of brown LSOA were deposited on fluorinated glass slides (Knopf, 2003) from the samples received from UCI using the tip of a needle (BD Precision Glide™ Needle, 0.9 mm x 40 mm). A dilute solution containing hydrophilic melamine beads (actual diameter:  $(0.87 \pm 0.04)$  µm, Sigma Aldrich, no. 86296) was then nebulized over the fluorinated glass slides containing the brown LSOA particles. This resulted in melamine beads being incorporated into the brown LSOA particles. The fluorinated glass slides containing the brown LSOA particles were then placed in a flow cell  
125 (Renbaum-Wolff et al., 2013b). The RH within the flow cell was controlled by passing a nitrogen carrier gas through a water bubbler, which was located in a temperature-controlled bath. The dew point of the nitrogen gas flow was measured with a hygrometer (General Eastern; Model 1311DR), and the temperature of the flow cell was measured with a thermocouple. From the dew point and the temperature of the flow cell, the RH was determined. The RH was calibrated at the beginning of each set of measurements using the deliquescence point of ammonium sulfate.

130

Once the fluorinated glass slides containing the brown LSOA particles were placed in the flow cell, a constant flow (1100 to 1200 sccm) of humidified nitrogen gas (Praxair, ultrapure) was passed over the brown LSOA particles, which caused a shear stress on the surface of the particles and circulation of the beads within the particles. The velocity of the beads was determined using an optical microscope (Zeiss Axio Observer). For each  $a_w$  studied, the speed of 7 to 16 beads in 2 to 5 brown LSOA droplets was measured and the bead speed was averaged. Once determined, the velocity of the beads was converted to viscosity using a calibration curve based on sucrose-water particles and glycerol-water particles from Grayson et al. (2017)(Grayson et al., 2017). Prior to measuring the velocity of the beads in an experiment, the brown LSOA particles were equilibrated with the RH within the flow cell for approximately 20 min, which should be long enough to ensure equilibration (Section S1).

Viscosity for the same brown LSOA at  $a_w$  of 0.05 and 0.3 are available from previous poke-flow measurements by Hinks et al. (2016). Briefly, in these studies brown LSOA was collected on hydrophobic glass surfaces using a procedure similar to the procedure described above. This resulted in supermicron particles with a spherical cap geometry. The particles were then poked with a sharp needle, generating a half-torus geometry. After poking, the material flowed and returned to its spherical cap geometry due to surface tension forces. From simulations of fluid flow, the viscosities of the material were determined. This technique is limited to viscosities  $\geq 10^3$  Pa s (Grayson et al., 2015). In addition, the upper and lower limits of viscosity from this technique differ by roughly a factor of 15 to 150. This uncertainty stems mainly from uncertainties in the parameters used when simulating the fluid flow.

## 2.3 Diffusion coefficient measurements

### 2.3.1 Generation of thin films of brown LSOA with a known $a_w$ for the diffusion coefficient measurements

Brown LSOA contains light absorbing molecules that are also fluorescent and easily photobleachable (Lee et al., 2013). Diffusion coefficients of these intrinsic fluorescent organic molecules were determined using rectangle area fluorescent recovery after photobleaching (discussed below). For this technique, thin films (20-90  $\mu\text{m}$  thick) containing brown LSOA with a known  $a_w$  were needed. To produce thin films of brown LSOA with a known  $a_w$ , particles of brown LSOA with diameters of 50-200  $\mu\text{m}$  were deposited on hydrophobic slides from the samples received from the UCI using the tip of a needle (BD Precision Glide<sup>TM</sup> Needle, 0.9 mm x 40 mm). The super-micrometer brown LSOA particles were then located within a flow cell or sealed glass jar with controlled RH to set the  $a_w$  within the brown LSOA (at equilibration,  $a_w$  within the brown LSOA equals RH/100). The times used to condition the brown LSOA particles to the controlled RH are given in Table S1, ranging from 17 min to 1.5 months, and discussed in Section S1. After equilibration, the brown LSOA particles were sandwiched between two hydrophobic glass slides to generate a thin film of brown LSOA with a thickness of 20-90  $\mu\text{m}$ . Assembly of the films occurred within a glove bag that had a RH set to match the RH used for conditioning the brown LSOA particles in order to ensure the  $a_w$  within the LSOA did not change during assembly of the films. The thickness of the films was controlled by aluminium spacers inserted between the two hydrophobic glass slides prior to assembly. After assembly, the brown LSOA

within the thin films were isolated from the surrounding atmosphere using a layer of vacuum grease around the perimeter of  
165 the films. For further details, see Chenyakin et al. (2017) and Fig. S1.

### 2.3.2 Measurements of diffusion coefficients

Fluorescence recovery after photobleaching (FRAP) has often been used to determine diffusion rates of fluorescent molecules  
in biological samples such as in the cytoplasm and nuclei of cells (Axelrod et al., 1976; Deschout et al., 2010; Jacobson et al.,  
1976; Meyvis et al., 1999; Seksek et al., 1997). To determine diffusion coefficients of the intrinsic fluorophores in the brown  
170 LSOA, we used a version of FRAP, referred to as rectangular area fluorescence recovery after photobleaching (rFRAP)  
(Deschout et al., 2010). rFRAP was chosen over circular FRAP, since rFRAP has a closed-form expression for the recovery  
process. In rFRAP, a rectangular region of a thin film containing fluorescent molecules is photobleached with a high intensity  
laser beam of a confocal laser scanning microscope (Fig S2). After photobleaching, the fluorescence signal within the  
photobleached region recovers due to diffusion of fluorescent molecules from outside the photobleached region into the  
175 photobleached region. The recovery of the fluorescence signal over time is monitored and used to determine the diffusion  
coefficient of the fluorescent molecules.

The rFRAP measurements were conducted with a laser scanning confocal microscope (Zeiss Axio Observer LSM 5 10 MP)  
with a low numerical aperture objective (Zeiss EC-Plan Neofluar 10x, 0.3 numerical aperture) to ensure near uniform  
180 photobleaching in the z-direction. One-dimensional scanning with a pixel dwell of 2.56  $\mu\text{s}$  and an image scan time of 1.57 s  
was used. The images were acquired with 512x512 pixels with a pinhole set to 80  $\mu\text{m}$ . The scanning laser power was varied  
between 17.0 to 42.6  $\mu\text{W}$  depending on the fluorescence of the sample. In order to achieve a bleach depth (decrease in  
fluorescence intensity) of 30-50 %, as suggested by Deschout et al. (2010) for rFRAP experiments, the laser power for  
photobleaching was varied between 93 and 297  $\mu\text{W}$ , depending on the sample (Deschout et al., 2010).

185 A rectangular area was used for photobleaching with length (x) and width (y). The recovery time in the rFRAP experiments  
were related to both the photobleaching area and diffusion rate. When the diffusion rate was fast (e.g. high water activities),  
we used a larger photobleaching area, and when the diffusion rate was slow (e.g. low water activities), we used a smaller  
photobleaching area to give experimentally accessible recovery times. The image sizes used in the rFRAP experiments were  
190 chosen in relation to the bleach size with larger image sizes used for larger bleach sizes. For example, at  $a_w \geq 0.8$ , photobleached  
areas of 20  $\mu\text{m}$  by 20  $\mu\text{m}$  and image sizes of 199.6  $\mu\text{m}$  by 199.6  $\mu\text{m}$  were used, while at  $a_w = 0.33$ , photobleached areas of 5  
 $\mu\text{m}$  by 5  $\mu\text{m}$  and 3  $\mu\text{m}$  by 3  $\mu\text{m}$  and image sizes of 30  $\mu\text{m}$  by 30  $\mu\text{m}$  were used. All rFRAP experiments were carried out at a  
temperature of 294.5 $\pm$ 1.0 K. Shown in Figure 1 are examples of images of brown LSOA films with  $a_w$  of 0.33, 0.6 and 0.9  
recorded during rFRAP experiments.

195 **2.3.3 Extraction of diffusion coefficients**

Based on Fick's second law of diffusion, Deschout et al. (2010) developed the following equation to describe the fluorescence intensities in thin films after photobleaching a rectangular area with a confocal microscope (Deschout et al., 2010):

$$\frac{F(x,y,t)}{F_0(x,y)} = 1 - \frac{K_0}{4} \left[ \operatorname{erf} \left( \frac{x + \frac{l_x}{2}}{\sqrt{w(D,t,r)}} \right) - \operatorname{erf} \left( \frac{x - \frac{l_x}{2}}{\sqrt{w(D,t,r)}} \right) \right] \times \left[ \operatorname{erf} \left( \frac{y + \frac{l_y}{2}}{\sqrt{w(D,t,r)}} \right) - \operatorname{erf} \left( \frac{y - \frac{l_y}{2}}{\sqrt{w(D,t,r)}} \right) \right], \quad (2)$$

where  $F(x, y, t)$  is the fluorescence intensity at coordinate  $(x, y)$  and time  $t$  after photobleaching,  $F_0(x, y)$  is the fluorescence  
 200 intensity at coordinate  $(x, y)$  prior to photobleaching,  $K_0$  is the effective bleach depth, which describes the decrease of the  
 fluorescence intensity within the photobleached area,  $l_x$  and  $l_y$  are the lengths of the photobleached area,  $r$  is the lateral  
 resolution of the microscope, and  $D$  is the diffusion coefficient of the fluorescent molecules. The parameter  $w(D, t, r)$  is given  
 by the following equation:

$$w(D, t, r) = r^2 + 4Dt. \quad (3)$$

205

In a first step of the analysis for the extraction of diffusion coefficients, the images recorded after photobleaching were  
 normalized to an image recorded prior to photobleaching using the open source program ImageJ (Schneider et al., 2012). The  
 resolution of the images was changed from 512x512 pixels to 128x128 pixels by averaging to reduce the noise. Then, Eq. 2  
 was used to extract  $w(D, t, r)$  from each image. In the fitting procedure used to extract  $w(D, t, r)$ ,  $K_0$  as well as a normalization  
 210 factor were left as free parameters. Next,  $w(D, t, r)$  was plotted as a function of  $t$  and a straight line was fit to the data. The  
 diffusion coefficient,  $D$ , was calculated from the slope of the straight line using a linear fit with Eq. (3). Examples of plots of  
 $w(D, t, r)$  vs  $t$  are shown in Figure 2.

Equation 2 assumes that the only mechanism for recovery in the photobleached region is diffusion of unbleached molecules.  
 The spontaneous recovery of the fluorescence signal without diffusion, referred to as reversible photobleaching, has been  
 215 observed in previous studies at short timescales (Sinnecker et al., 2005; Stout and Axelrod, 1995; Verkman, 2003). To determine  
 if this process occurred during our diffusion measurements with brown LSOA, a separate set of experiments was carried out.  
 Particles of brown LSOA (40 to 90  $\mu\text{m}$  in diameter) were conditioned to an  $a_w$  of 0.6 and the entire particle was photobleached  
 until the fluorescence intensity decreased by between 17 and 47%. The photobleaching was performed across the entire particle  
 in order to rule out fluorescence intensity recovery due to diffusion of fluorescent molecules. Within the first five seconds after  
 220 photobleaching a small amount of the fluorescent signal recovered (1-3 % of the photobleached signal), which we attribute to  
 reversible photobleaching. To ensure this process did not impact our diffusion measurements, the data recorded during the first  
 five seconds after photobleaching in the rFRAP experiments were not included when determining diffusion coefficients.

Possible heating of the sample during photobleaching by the laser was not expected to impact the diffusion measurements  
 since local heating during photobleaching should be dissipated to the surroundings much faster than the time of the diffusion  
 225 measurements. Nevertheless, to support this expectation, two experiments were carried out with different laser intensities but  
 on the same sample conditioned to an  $a_w$  to 0.9. A laser intensity of 139.9  $\mu\text{W}$  was used for a bleach depth of 20% and a laser

intensity of 330  $\mu\text{W}$  was used for a bleach depth of 50%. Within uncertainty, the diffusion coefficients determined with both bleach depths were in agreement:  $(2.5\pm 0.5)\cdot 10^{-9} \text{ cm}^2 \text{ s}^{-1}$  was obtained for a laser intensity of 139.9  $\mu\text{W}$  and  $(2.8\pm 0.1)\cdot 10^{-9} \text{ cm}^2 \text{ s}^{-1}$  for a diffusion coefficient was obtained for a laser intensity of 330  $\mu\text{W}$  (uncertainties correspond to 95 % confidence intervals).

Equation 2 assumes that the fluorescence intensity is proportional to the concentration of the intrinsic fluorescent molecules, which is a valid assumption when the transmittance of light through the samples is  $\geq 95\%$  (Fonin et al., 2014). In our experiments the transmittance of light through the samples was  $\leq 93\%$ . To take into account the non-linearity between the fluorescence signal and concentration, the measured fluorescence signal was first converted to concentration using the following equation:

$$\frac{C(x,y,t)}{C_0(x,y)} = \frac{\log\left[1 - (1 - T_0) \frac{F(x,y,t)}{F_0(x,y)}\right]}{\log(T_0)}, \quad (4)$$

where  $\frac{C(x,y,t)}{C_0(x,y)}$  is the normalized concentration of the intrinsic fluorescent dye,  $\frac{F(x,y,t)}{F_0(x,y)}$  is the normalized fluorescence signal, and  $T_0$  is the transmittance prior to the photobleaching process. Equation 4 is derived in Section S2. After the normalized concentrations were calculated, they were used in Eq. 2 in place of the normalized fluorescence signal. Note, the application of Eq. 4 to account for non-linearity between the fluorescence signal and concentration changed the diffusion coefficients by less than the uncertainties in the measurements.

### 3 Results and Discussion

#### 3.1 Viscosity of brown limonene SOA

Figure 3 shows the viscosity of brown LSOA as a function of  $a_w$  measured with the bead-mobility technique. For comparison, the known viscosity of pure water and the viscosity of brown LSOA measured previously using the poke-and-flow technique are also included (Hinks et al., 2016). Overall, Figure 3 shows that the viscosity increases by 3-5 orders of magnitude as the  $a_w$  decreases from 0.9 to approximately 0.05. An increase in viscosity with a decrease in  $a_w$  is expected due to the plasticizing effect of water (Koop et al., 2011; Power et al., 2013; Zobrist et al., 2011). A liquid has a viscosity of  $< 10^2 \text{ Pa}\cdot\text{s}$ , a semisolid has a viscosity of  $10^2$  and  $10^{12} \text{ Pa}\cdot\text{s}$ , and an amorphous solid has a viscosity of  $> 10^{12} \text{ Pa}\cdot\text{s}$  (Koop et al., 2011; Mikhailov et al., 2009; Shiraiwa et al., 2011). Based on Figure 3, the brown LSOA studied here can be considered as a liquid above a  $a_w$  of 0.7, and as a semisolid at  $a_w$  below roughly 0.5.

#### 3.1 Diffusion coefficients and mixing times of intrinsic fluorophores in brown limonene SOA

Figure 4(a) shows the measured diffusion coefficients of the intrinsic fluorophores in brown LSOA as a function of  $a_w$ . The average diffusion coefficient decreases from  $5.5\cdot 10^{-9} \text{ cm}^2/\text{s}$  to  $7.1\cdot 10^{-13} \text{ cm}^2/\text{s}$  as the  $a_w$  decreases from 0.9 to 0.33. The strong dependence on  $a_w$  is due to the plasticizing effect of water as mentioned above (Koop et al., 2011; Power et al., 2013; Zobrist

et al., 2011). Also included in Figure 4 (secondary y-axis) is the mixing time of the intrinsic fluorophores by molecular diffusion within a 200 nm brown SOA particle based on the measured diffusion coefficients. Mixing times were calculated with the following equation (Seinfeld and Pandis, 2016; Shiraiwa et al., 2011):

$$\tau_{mixing} = \frac{D_p^2}{4\pi^2 D_{org}}, \quad (5)$$

260 where  $D_p$  is the diameter of the particle and  $D_{org}$  the measured diffusion coefficient of the intrinsic fluorophore. The mixing time is the time after which the concentration of the diffusing molecules at the centre of the particle deviates by less than 1/e from the equilibrium concentration (Shiraiwa et al., 2011). Based on the measured diffusion coefficients, for the brown LSOA studied here mixing times of the organics within 200 nm particles range from 0.002 s to 14 s for  $a_w$  from 0.9 to 0.33.

265 Also shown in Figure 4 is the frequency distributions of  $a_w$  (Panel b) and temperatures (Panel c) found in the planetary boundary layer (PBL) for the months of January and July. We calculated these frequency distributions using GEOS-Chem version v10-01 (Pye et al., 2010), which was driven by 6-hr average GEOS-5 meteorology fields. Following Maclean et al. (2017), when determining the frequency distributions of  $a_w$  and temperatures within the PBL, we only included grid cells in a column up to the top of the PBL if the monthly averaged concentrations of organic aerosol (OA) were  $> 0.5 \mu\text{g m}^{-3}$  at the surface, based on  
270 GEOS-Chem version v10-01 (Pye et al., 2010). Based on this model, OA concentrations were almost always  $< 0.5 \mu\text{g m}^{-3}$  above the surface of the oceans. Hence, Fig. 4 b-c do not include most conditions over the oceans. We excluded cases when OA concentrations were  $< 0.5 \mu\text{g m}^{-3}$  at the surface since these concentrations are not expected to be important for climate or health. OA concentrations were  $> 0.5 \mu\text{g m}^{-3}$  in all but one of the previous surface measurements of OA at remote locations (Spracklen et al., 2011).

275

Figure 4(b) shows that  $a_w$  in the PBL is most often  $\geq 0.33$  when the organic mass concentrations are higher than  $0.5 \mu\text{g m}^{-3}$  at the surface. Figure 4(c) shows that the temperature in the PBL is often within 5 K of the temperature used in our experiments (294.5 K). Based on Figure 4, mixing times of intrinsic fluorophore in the brown LSOA studied here are often short ( $< 1$  h) for  $a_w$ -values and temperatures most often found in the PBL when the organic mass concentrations are higher than  $0.5 \mu\text{g m}^{-3}$ .

280

The diffusion coefficients and mixing times reported here correspond to brown LSOA generated using mass concentrations of  $1,000 \mu\text{g m}^{-3}$  in a flow reactor. For some types of SOA (SOA from ozonolysis of  $\alpha$ -pinene, limonene, 3-hexenyl acetate and 3-hexen-1-ol) the viscosity of the SOA increases as the mass concentration used to generate the SOA decreases (Grayson et al., 2016b; Jain et al., 2018). Since mass concentrations of biogenic SOA particles found in the atmosphere are most often  
285  $\leq 10 \mu\text{g m}^{-3}$  (Spracklen et al., 2011) the values reported here likely represent the lower limit for the viscosities and upper limit for the diffusion coefficients. Additional studies are needed to determine diffusion coefficients and mixing times for more atmospherically relevant mass concentrations. In addition, the brown LSOA were generated using a ratio of limonene to ozone

~1, which suggests than not all double bonds in limonene were oxidized. Additional studies are also needed to determine if diffusion coefficients in brown LSOA are sensitive to the extent of oxidation of LSOA molecules.

290

Ye et al. (2018) studied the timescale for mixing of organics from toluene oxidation within limonene SOA particles using mass spectrometry (Ye et al., 2018). In these studies, the limonene SOA particles were generated with mass concentration of 16-22  $\mu\text{g m}^{-3}$ . Based on the studies by Ye et al. (2018) the mixing times of organics within limonene SOA particles is on the order of 3-4 hr for RH values ranging from 10 to 30%, with little evidence for an RH dependence. At 33% RH, we calculate a mixing time of approximately 14 s. This corresponds to a difference in diffusion coefficients of a factor of roughly 1000. A possible explanation for the apparent difference between the current results and the results reported by Ye et al. (2018) is the difference in the mass concentrations used to generate the SOA, and the low extent of oxidation of LSOA compounds, as discussed above.

### 300 **3.4. Comparison between measured diffusion coefficients and Stokes-Einstein predictions**

Shown in Figure 5 are the measured diffusion coefficients and predicted diffusion coefficients based on viscosity measurements and the Stokes-Einstein relation. The viscosity measurements include our new bead-mobility viscosity results (Figure 3) and previous poke-flow viscosity measurements by Hinks et al. (2016), as well as viscosity measurements of pure water for comparison (Crittenden et al., 2012;Hinks et al., 2016). To predict diffusion coefficients from the viscosity measurements and the Stokes-Einstein equation, the average dimension of the intrinsic fluorophores is needed. The exact molecular identities of the chromophores and fluorophores in brown LSOA is not known. Previous studies suggest that there is a distribution of chromophores with a broad range of molecular weights of the order of 500 g/mol (Nguyen et al., 2013). Therefore, we tested a range of molecular weights from 300 to 800 g/mol, corresponding to hydrodynamic radii from 4.5 to 6.2 Å with an assumed density of 1.3 g/cm<sup>3</sup> (Saathoff et al., 2009), and an assumed spherical geometry of the intrinsic fluorophores.

Figure 5 shows that the difference between the measured and predicted diffusion coefficients is less than the uncertainty of the measurements for diffusion coefficients as small as roughly  $10^{-12} \text{ cm}^2 \text{ s}^{-1}$ , which corresponds to a viscosity of between  $4 \cdot 10^2$  to  $1.2 \cdot 10^4 \text{ Pa} \cdot \text{s}$ , based on Figure 4. This conclusion is consistent with most previous studies that have investigated the accuracy of the Stokes-Einstein relation for predicting diffusion coefficients of large organic molecules in organic-water mixtures. For example, Chenyakin et al. (2017), Champion et al. (1997), and Price et al. (2016) showed that the Stokes-Einstein relation predicts diffusion coefficients of large organics in sucrose-water solution consistent with measurements (i.e., within the uncertainty of the measurements) when the viscosity is  $\lesssim 1 \cdot 10^4 \text{ Pa} \cdot \text{s}$  (Champion et al., 1997;Chenyakin et al., 2017;Price et al., 2016). In contrast, Longinotti and Corti (2007) and Corti et al. (2008) found disagreement between measured and predicted

315

320 diffusion coefficients of large organics in organic-water solutions at slightly lower viscosities (Corti et al., 2008; Longinotti and Corti, 2007).

#### 4 Summary and conclusion

325 One physicochemical property of SOA particles that remains poorly understood is diffusion rates of representative organics within SOA particles. To estimate diffusion rates of organics in realistic models for SOA particles, we (as well as other researchers) have used viscosity measurements together with the Stokes-Einstein relation. Until now, the accuracy of the Stokes-Einstein relation for predicting diffusion coefficients of organics in SOA particles had not been quantified, leading to uncertainties when estimating diffusion rates from viscosity measurements. In this study, we measured the viscosity of brown LSOA using the bead mobility technique. From these viscosity values, we calculated diffusion coefficients of large organic molecules in brown LSOA. These calculated diffusion coefficient values were compared to diffusion coefficients of large organic molecules that were measured directly in brown LSOA using fluorescence recovery after photobleaching. We found that the Stokes-Einstein relation gives diffusion coefficients within the uncertainty of the measurements for brown LSOA matrices with viscosities between  $0.2 \text{ Pa} \cdot \text{s}$  and  $1.2 \cdot 10^4 \text{ Pa} \cdot \text{s}$ .

335 In addition, mixing times in a 200 nm sized brown LSOA particle were calculated based on the measured diffusion coefficients. Mixing times were found to vary between 0.001 s at an  $a_w$  of 0.9 and 14 s at an  $a_w$  of 0.3. These results suggest that the mixing times of large organics in the brown LSOA studied here are short ( $< 1 \text{ h}$ ) for  $a_w$  and temperatures often found in the PBL. However, since the mixing times reported here correspond to brown LSOA generated using mass loadings of  $1,000 \mu\text{g m}^{-3}$ , the mixing times are likely to be longer in ambient biogenic SOA particles typically found at mass loadings below  $10 \mu\text{g m}^{-3}$  (Spracklen et al., 2011). Additional studies are needed using more atmospherically relevant mass concentrations, as well as utilizing a range of oxidation conditions from “fresh” to “highly-aged” SOA. The measurements reported here can be extended to lower mass loading conditions by using a multi-orifice impactor, which concentrates collected material into spots, and by collecting material for extended periods of time (e.g. several days) (Grayson et al., 2016a).

#### 5 Acknowledgement

345 This work was funded by the Natural Science and Engineering Research Council of Canada. JLJ was supported by DOE (BER/ASR) DE-SC0016559. Support from the MJ Murdock Charitable Trust (grant 2012183) for computing infrastructure at Portland State University is acknowledged.

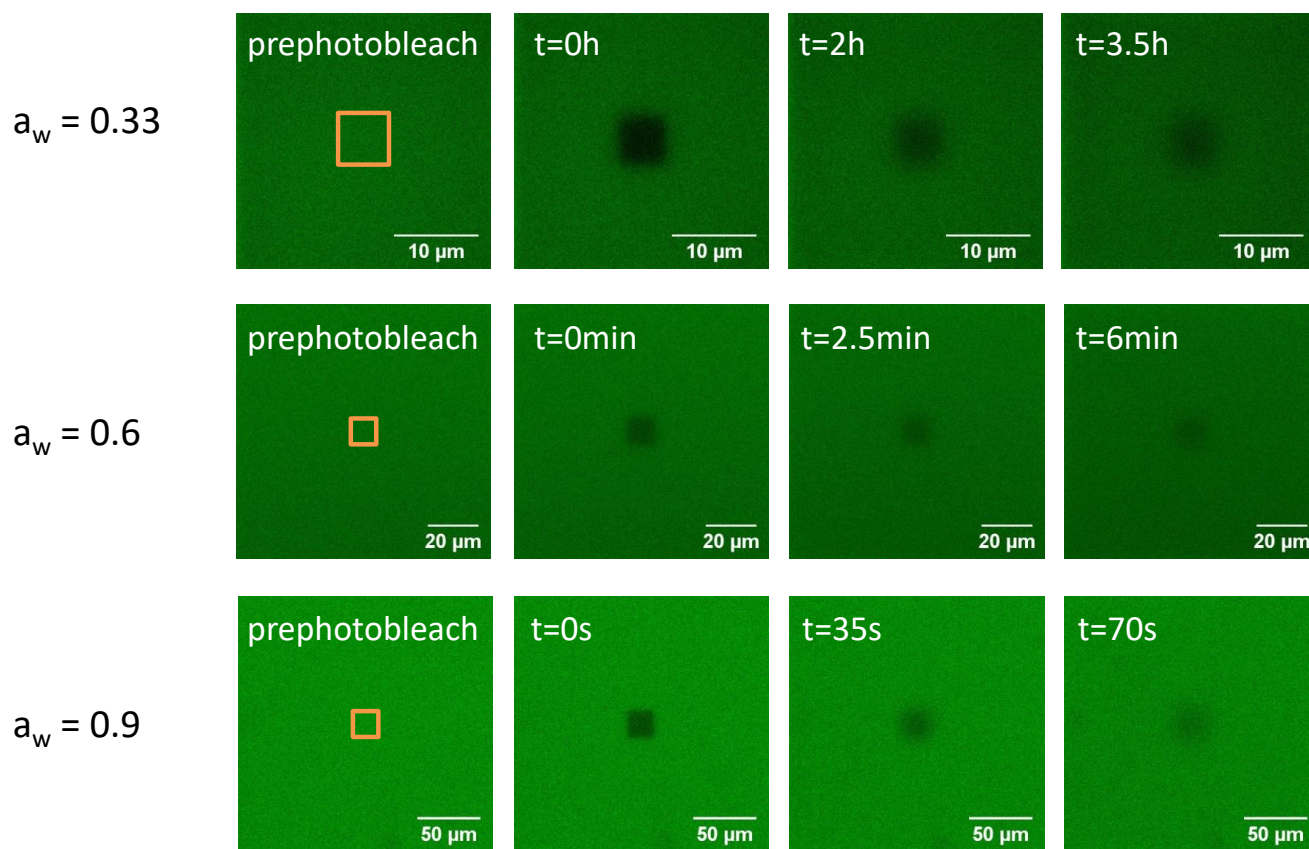
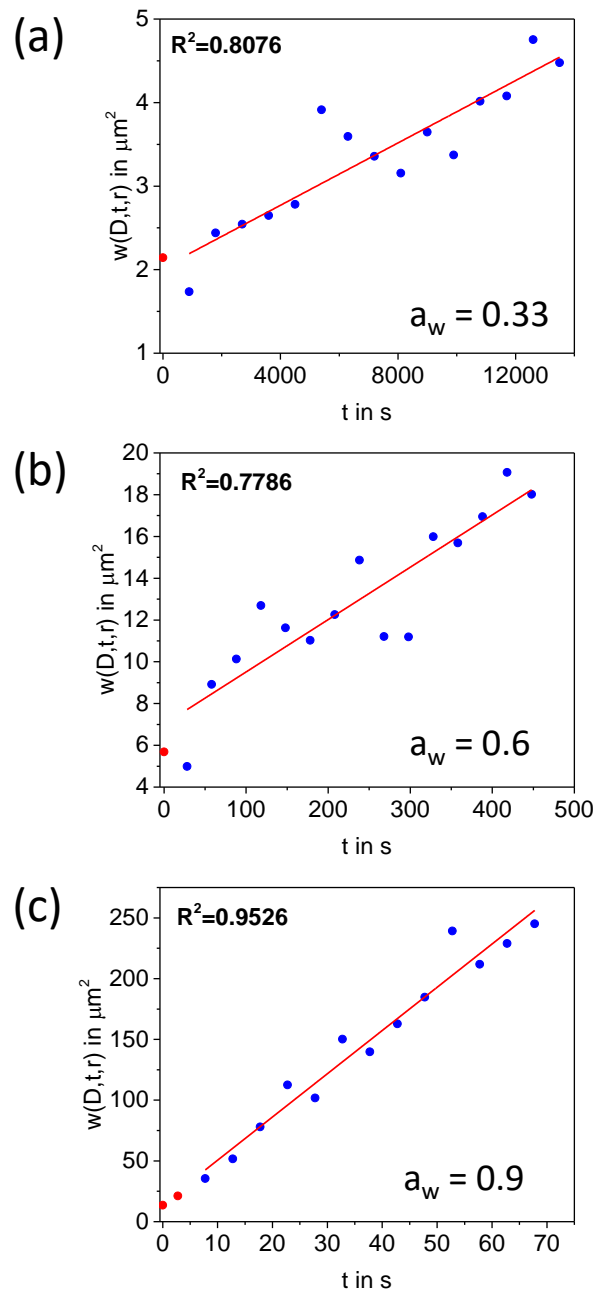


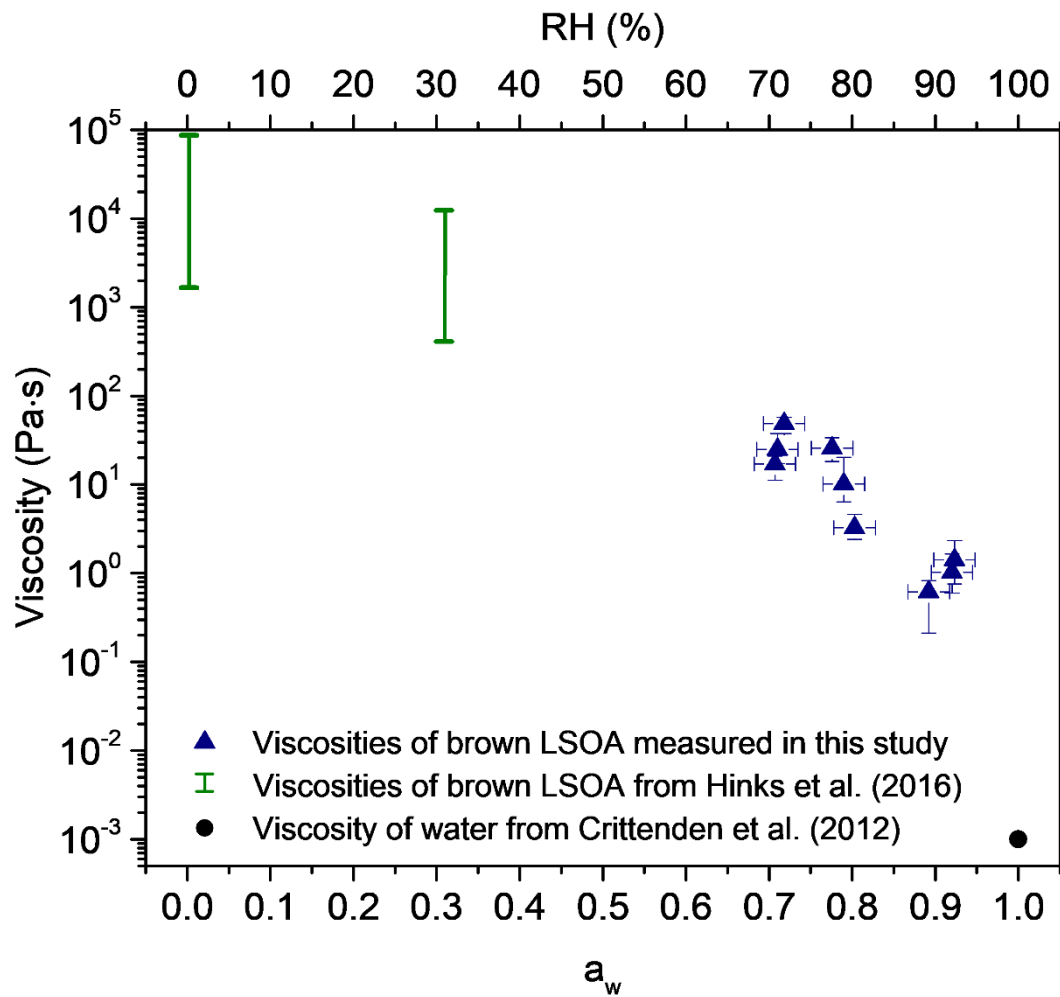
**Figure 1: Images of brown limonene SOA films at three different  $a_w$  (0.33, 0.6 and 0.9) recorded during a rectangular fluorescence recovery after photobleaching (rFRAP) experiment. Times shown in each panel correspond to times after photobleaching. The orange rectangles depict the area to be photobleached.**



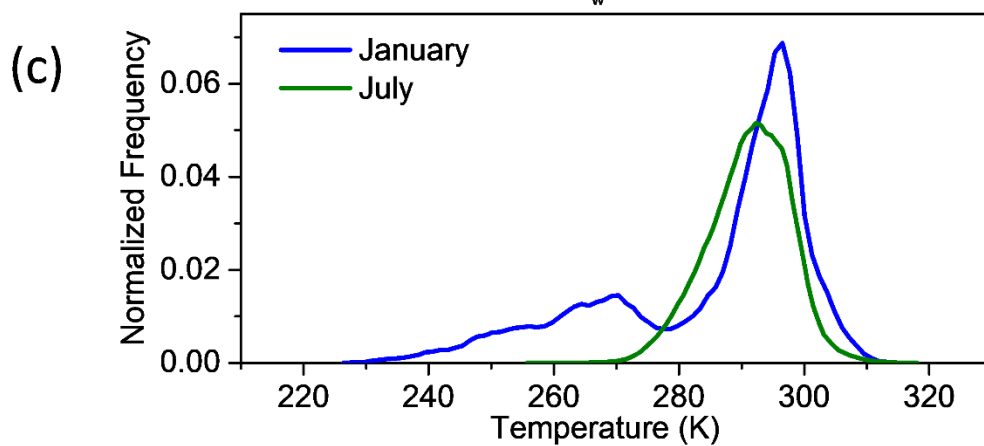
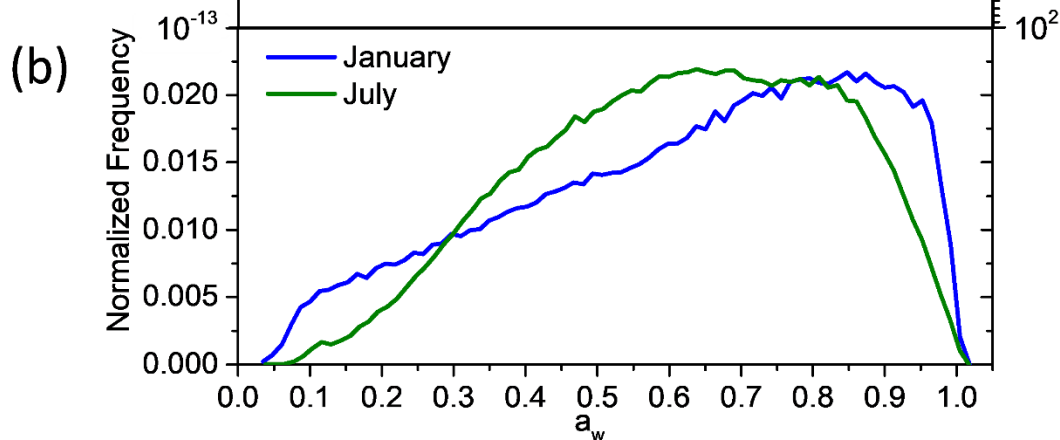
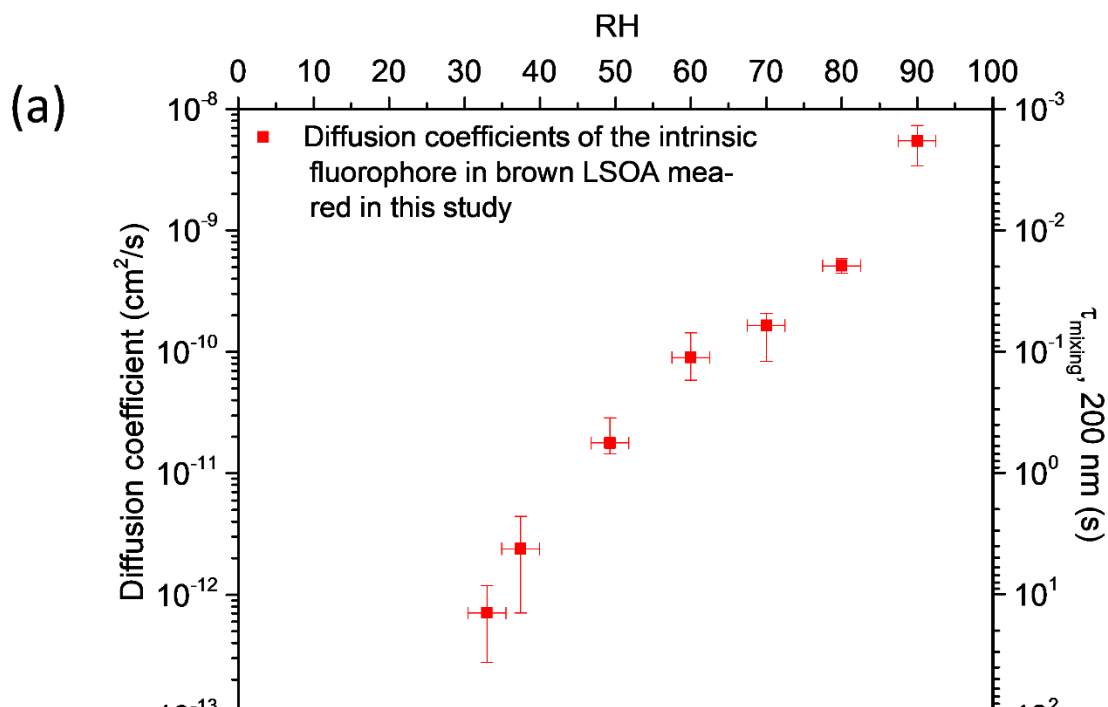
355

**Figure 2: Plot of  $w(D,t,r)$  as a function of time at  $a_w$  of 0.9, 0.6 and 0.33. The red line is a linear fit to the data. The blue circles represent the data points that were included in the linear fit, the red circles represent data that were not included because of possible reversible photobleaching. The diffusion coefficients were obtained from the slopes.**

360

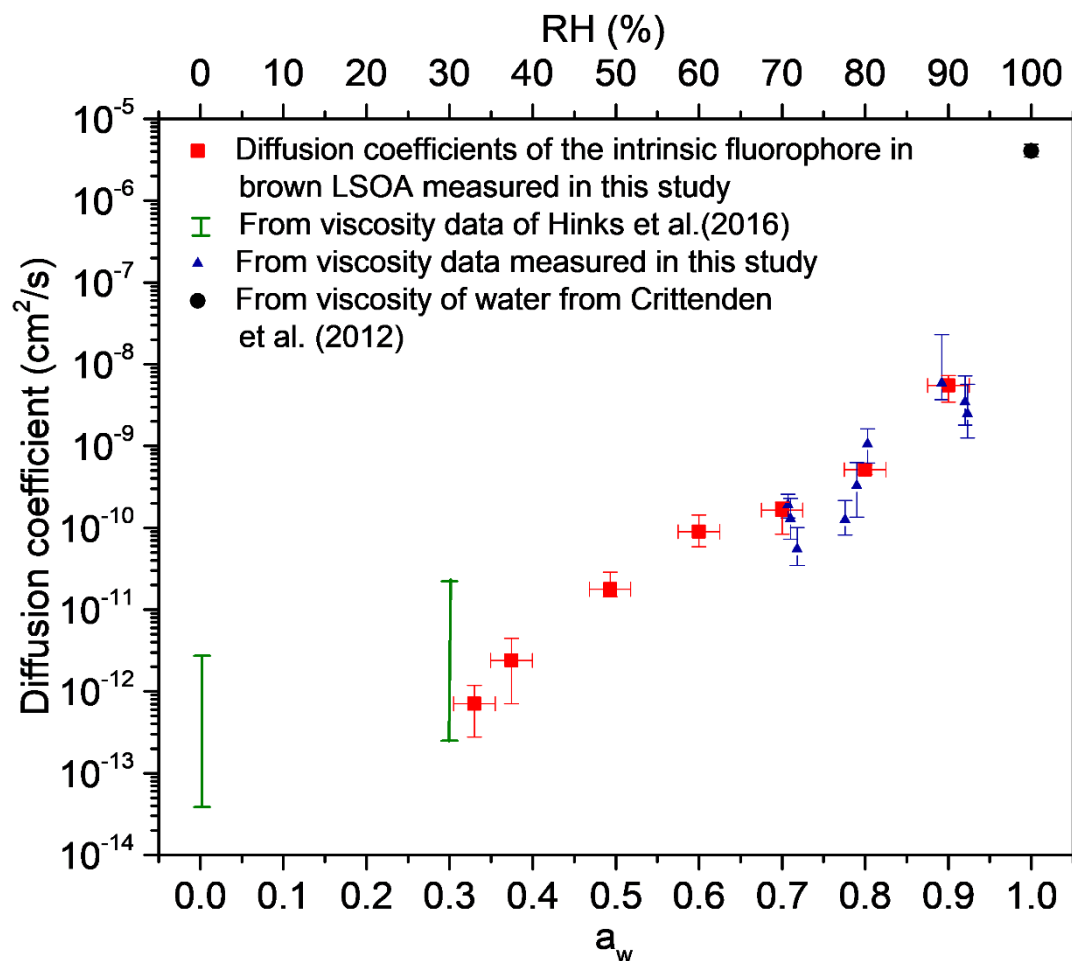


365 Figure 3: Viscosity of brown LSOA as a function of  $a_w$  (primary x-axis) and RH (secondary x-axis). The green bars show the viscosities that were measured by Hinks et al. (2016) and the blue triangles show the viscosities that were measured in this study using the bead mobility technique. The black circle is the viscosity of water measured by Crittenden et al. (2012).



370 **Figure 4: Panel (a):** measured diffusion coefficients of the intrinsic fluorophore in brown LSOA as a function of  $a_w$  (primary x-axis) and RH (secondary x-axis). The secondary y-axis shows the mixing time, which is the time that would be needed for intrinsic fluorophores to mix within a 200 nm brown limonene particle. The y-error bars correspond to the highest and lowest diffusion coefficient measured. The x-error bars correspond to uncertainty of the RH measurements ( $\pm 2.5\%$ ). **Panel (b):** the  $a_w$  distribution in January (blue line) and July (green line) in the planetary boundary layer (PBL) when monthly averaged concentrations of organic aerosol (OA) are  $>0.5 \mu\text{g m}^{-3}$  at the surface based on GEOS-Chem. **Panel (c)** the temperature distribution in January and July in the PBL when monthly averaged concentrations of OA are  $>0.5 \mu\text{g m}^{-3}$  at the surface based on GEOS-Chem.

375



385 **Figure 5: Measured and calculated diffusion coefficients in brown LSOA as a function of  $a_w$  (primary x-axis) and RH (secondary x-axis). The red squares show the measured diffusion coefficients of intrinsic fluorophores in brown LSOA. The blue triangles show**  
 390 **the calculated diffusion coefficients of the intrinsic fluorophore in brown LSOA based on viscosities measured in this study using the bead mobility technique and the Stokes-Einstein equation. The y-error bars for the diffusion coefficients measured in this study (red squares) and the diffusion coefficients calculated from bead mobility viscosity measurements (blue triangles) show the highest and lowest values measured. The green vertical bars depict the highest and the lowest limit of calculated diffusion coefficients of brown LSOA based on viscosity measurements from Hinks et al. (2016) and the Stokes-Einstein equation. The black circle depicts the calculated diffusion coefficient of the intrinsic fluorophore in pure water based on viscosity measurements of Crittenden et al. (2012) and the Stokes-Einstein equation. The uncertainties for the calculated diffusion coefficients take into account the uncertainty of the hydrodynamic radii of the diffusing molecules (4.5 to 6.2 Å).**

## References

- Adler, G., Koop, T., Haspel, C., Taraniuk, I., Moise, T., Koren, I., Heiblum, R. H., and Rudich, Y.: Formation of highly porous aerosol particles by atmospheric freeze-drying in ice clouds, *Proceedings of the National Academy of Sciences*, 110, 20414-20419, 10.1073/pnas.1317209110, 2013.
- Axelrod, D., Koppel, D. E., Schlessinger, J., Elson, E., and Webb, W. W.: Mobility measurement by analysis of fluorescence photobleaching recovery kinetics, *Biophysical Journal*, 16, 1055-1069, 10.1016/S0006-3495(76)85755-4, 1976.
- Baltensperger, U., Dommen, J., Alfarra, M. R., Duplissy, J., Gaeggeler, K., Metzger, A., Facchini, M. C., Decesari, S., Finessi, E., and Reining, C.: Combined determination of the chemical composition and of health effects of secondary organic aerosols: the POLYSOA project, *Journal of aerosol medicine and pulmonary drug delivery*, 21, 145-154, 10.1089/jamp.2007.0655, 2008.
- Bastelberger, S., Krieger, U. K., Luo, B., and Peter, T.: Diffusivity measurements of volatile organics in levitated viscous aerosol particles, *Atmos. Chem. Phys.*, 17, 8453-8471, 10.5194/acp-17-8453-2017, 2017.
- Bateman, A. P., Bertram, A. K., and Martin, S. T.: Hygroscopic Influence on the Semisolid-to-Liquid Transition of Secondary Organic Materials, *The Journal of Physical Chemistry A*, 119, 4386-4395, 10.1021/jp508521c, 2015.
- Booth, A. M., Murphy, B., Riipinen, I., Percival, C. J., and Topping, D. O.: Connecting Bulk Viscosity Measurements to Kinetic Limitations on Attaining Equilibrium for a Model Aerosol Composition, *Environmental Science & Technology*, 48, 9298-9305, 10.1021/es501705c, 2014.
- Boyd, C. M., Nah, T., Xu, L., Berkemeier, T., and Ng, N. L.: Secondary Organic Aerosol (SOA) from Nitrate Radical Oxidation of Monoterpenes: Effects of Temperature, Dilution, and Humidity on Aerosol Formation, Mixing, and Evaporation, *Environmental Science & Technology*, 51, 7831-7841, 10.1021/acs.est.7b01460, 2017.
- Champion, D., Hervet, H., Blond, G., Le Meste, M., and Simatos, D.: Translational Diffusion in Sucrose Solutions in the Vicinity of Their Glass Transition Temperature, *The Journal of Physical Chemistry B*, 101, 10674-10679, 10.1021/jp971899i, 1997.
- Chenyakin, Y., Ullmann, D. A., Evoy, E., Renbaum-Wolff, L., Kamal, S., and Bertram, A. K.: Diffusion coefficients of organic molecules in sucrose-water solutions and comparison with Stokes-Einstein predictions, *Atmos. Chem. Phys.*, 17, 2423-2435, 10.5194/acp-17-2423-2017, 2017.
- Chu, Y., and Chan, C. K.: Reactive Uptake of Dimethylamine by Ammonium Sulfate and Ammonium Sulfate-Sucrose Mixed Particles, *The Journal of Physical Chemistry A*, 121, 206-215, 10.1021/acs.jpca.6b10692, 2017.
- Clegg, S. L., Brimblecombe, P., and Wexler, A. S.: Thermodynamic Model of the System  $\text{H}^+ - \text{NH}_4^+ - \text{SO}_4^{2-} - \text{NO}_3^- - \text{H}_2\text{O}$  at Tropospheric Temperatures, *The Journal of Physical Chemistry A*, 102, 2137-2154, 10.1021/jp973042r, 1998.
- Corti, H. R., Frank, G. A., and Marconi, M. C.: An Alternate Solution of Fluorescence Recovery Kinetics after Spot-Bleaching for Measuring Diffusion Coefficients. 2. Diffusion of Fluorescein in Aqueous Sucrose Solutions, *Journal of Solution Chemistry*, 37, 1593-1608, 10.1007/s10953-008-9329-4, 2008.
- Crittenden, J. C., Trussell, R. R., Hand, D. W., Howe, K. J., and Tchobanoglous, G.: Physical and Chemical Quality of Water, in: *MWH's Water Treatment: Principles and Design*, Third Edition, John Wiley & Sons, Inc., 17-71, 2012.
- Davies, J. F., and Wilson, K. R.: Nanoscale interfacial gradients formed by the reactive uptake of OH radicals onto viscous aerosol surfaces, *Chemical Science*, 6, 7020-7027, 10.1039/c5sc02326b, 2015.
- Deschout, H., Hagman, J., Fransson, S., Jonasson, J., Rudemo, M., Lorén, N., and Braeckmans, K.: Straightforward FRAP for quantitative diffusion measurements with a laser scanning microscope, *Opt. Express*, 18, 22886-22905, 10.1364/oe.18.022886, 2010.
- Fonin, A. V., Sulatskaya, A. I., Kuznetsova, I. M., and Turoverov, K. K.: Fluorescence of Dyes in Solutions with High Absorbance. Inner Filter Effect Correction, *PLoS ONE*, 9, e103878, 10.1371/journal.pone.0103878, 2014.

- 440 Grayson, J. W., Song, M., Sellier, M., and Bertram, A. K.: Validation of the poke-flow technique combined with simulations of fluid flow for determining viscosities in samples with small volumes and high viscosities, *Atmos. Meas. Tech.*, 8, 2463-2472, 10.5194/amt-8-2463-2015, 2015.
- Grayson, J. W., Zhang, Y., Mutzel, A., Renbaum-Wolff, L., Boege, O., Kamal, S., Herrmann, H., Martin, S. T., and Bertram, A. K.: Effect of varying experimental conditions on the viscosity of alpha-pinene derived secondary organic material, *Atmospheric Chemistry and Physics*, 16, 6027-6040, 10.5194/acp-16-6027-2016, 2016a.
- 445 Grayson, J. W., Zhang, Y., Mutzel, A., Renbaum-Wolff, L., Böge, O., Kamal, S., Herrmann, H., Martin, S. T., and Bertram, A. K.: Effect of varying experimental conditions on the viscosity of  $\alpha$ -pinene derived secondary organic material, *Atmos. Chem. Phys.*, 16, 6027-6040, 10.5194/acp-16-6027-2016, 2016b.
- Grayson, J. W., Evoy, E., Song, M., Chu, Y., Maclean, A., Nguyen, A., Upshur, M. A., Ebrahimi, M., Chan, C. K., Geiger, F. M., Thomson, R. J., and Bertram, A. K.: The effect of hydroxyl functional groups and molar mass on the viscosity of non-crystalline organic and organic-water particles, *Atmos. Chem. Phys.*, 17, 8509-8524, 10.5194/acp-17-8509-2017, 2017.
- Gržinić, G., Bartels-Rausch, T., Berkemeier, T., Türler, A., and Ammann, M.: Viscosity controls humidity dependence of N<sub>2</sub>O<sub>5</sub> uptake to citric acid aerosol, *Atmos. Chem. Phys.*, 15, 13615-13625, 10.5194/acp-15-13615-2015, 2015.
- Hallquist, M., Wenger, J. C., Baltensperger, U., Rudich, Y., Simpson, D., Claeys, M., Dommen, J., Donahue, N. M., George, C., Goldstein, A. H., Hamilton, J. F., Herrmann, H., Hoffmann, T., Iinuma, Y., Jang, M., Jenkin, M. E., Jimenez, J. L., Kiendler-Scharr, A., Maenhaut, W., McFiggans, G., Mentel, T. F., Monod, A., Prévôt, A. S. H., Seinfeld, J. H., Surratt, J. D., Szmigielski, R., and Wildt, J.: The formation, properties and impact of secondary organic aerosol: current and emerging issues, *Atmos. Chem. Phys.*, 9, 5155-5236, 10.5194/acp-9-5155-2009, 2009.
- Hildebrandt Ruiz, L., Paciga, A., Cerully, K., Nenes, A., Donahue, N., and Pandis, S.: Formation and aging of secondary organic aerosol from toluene: changes in chemical composition, volatility, and hygroscopicity, *Atmospheric Chemistry and Physics*, 15, 8301-8313, 10.5194/acp-15-8301-2015, 2015.
- 460 Hinks, M. L., Brady, M. V., Lignell, H., Song, M., Grayson, J. W., Bertram, A. K., Lin, P., Laskin, A., Laskin, J., and Nizkorodov, S. A.: Effect of viscosity on photodegradation rates in complex secondary organic aerosol materials, *Physical Chemistry Chemical Physics*, 18, 8785-8793, 10.1039/C5CP05226B, 2016.
- 465 Hosny, N. A., Fitzgerald, C., Tong, C., Kalberer, M., Kuimova, M. K., and Pope, F. D.: Fluorescent lifetime imaging of atmospheric aerosols: a direct probe of aerosol viscosity, *Faraday Discussions*, 165, 343-356, 10.1039/c3fd00041a, 2013.
- Houle, F. A., Hinsberg, W. D., and Wilson, K. R.: Oxidation of a model alkane aerosol by OH radical: the emergent nature of reactive uptake, *Physical Chemistry Chemical Physics*, 17, 4412-4423, 10.1039/c4cp05093b, 2015.
- Huff Hartz, K. E., Rosenørn, T., Ferchak, S. R., Raymond, T. M., Bilde, M., Donahue, N. M., and Pandis, S. N.: Cloud condensation nuclei activation of monoterpene and sesquiterpene secondary organic aerosol, *Journal of Geophysical Research: Atmospheres*, 110, n/a-n/a, 10.1029/2004jd005754, 2005.
- 470 Jacobson, K., Wu, E., and Poste, G.: Measurement of the translation mobility of concanavalin a in glycerol-saline solutions and on the cell surface by fluorescence recovery after photobleaching, *Biochimica et Biophysica Acta (BBA) - Biomembranes*, 433, 215-222, 10.1016/0005-2736(76)90189-9, 1976.
- 475 Jain, S., Fischer, K. B., and Petrucci, G. A.: The Influence of Absolute Mass Loading of Secondary Organic Aerosols on Their Phase State, *Atmosphere*, 9, 10.3390/atmos9040131, 2018.
- Jang, M., Ghio, A. J., and Cao, G.: Exposure of BEAS-2B Cells to Secondary Organic Aerosol Coated on Magnetic Nanoparticles, *Chemical research in toxicology*, 19, 1044-1050, 10.1021/tx0503597, 2006.
- Jimenez, J. L., Canagaratna, M. R., Donahue, N. M., Prevot, A. S. H., Zhang, Q., Kroll, J. H., DeCarlo, P. F., Allan, J. D., Coe, H., Ng, N. L., Aiken, A. C., Docherty, K. S., Ulbrich, I. M., Grieshop, A. P., Robinson, A. L., Duplissy, J., Smith, J. D., Wilson, K. R., Lanz, V. A., Hueglin, C., Sun, Y. L., Tian, J., Laaksonen, A., Raatikainen, T., Rautiainen, J., Vaattovaara, P., Ehn, M., Kulmala, M., Tomlinson, J. M., Collins, D. R., Cubison, M. J., Dunlea, J., Huffman, J. A., Onasch, T. B., Alfarra, M. R., Williams, P. I., Bower, K., Kondo, Y., Schneider, J., Drewnick, F., Borrmann, S., Weimer, S., Demerjian, K., Salcedo, D., Cottrell, L., Griffin, R., Takami, A., Miyoshi, T., Hatakeyama, S., Shimojo, A., Sun, J. Y., Zhang, Y. M., Dzepina, K., Kimmel, J. R., Sueper, D., Jayne, J. T., Herndon, S. C., Trimborn, A. M., Williams, L. R., Wood, E. C., Middlebrook, A. M., Kolb, C. E., Baltensperger, U., and Worsnop, D. R.: Evolution of Organic Aerosols in the Atmosphere, *Science*, 326, 1525-1529, 10.1126/science.1180353, 2009.
- Kanakidou, M., Seinfeld, J. H., Pandis, S. N., Barnes, I., Dentener, F. J., Facchini, M. C., Van Dingenen, R., Ervens, B., Nenes, A., Nielsen, C. J., Swietlicki, E., Putaud, J. P., Balkanski, Y., Fuzzi, S., Horth, J., Moortgat, G. K., Winterhalter, R., Myhre,

- 490 C. E. L., Tsigaridis, K., Vignati, E., Stephanou, E. G., and Wilson, J.: Organic aerosol and global climate modelling: a review, *Atmos. Chem. Phys.*, 5, 1053-1123, 10.5194/acp-5-1053-2005, 2005.
- Knopf, D. A.: Thermodynamic properties and nucleation processes of upper tropospheric and lower stratospheric aerosol particles, Diss. ETH No. 15103, Zurich, Switzerland, 2003.
- Koop, T., Kapilashrami, A., Molina, L. T., and Molina, M. J.: Phase transitions of sea-salt/water mixtures at low temperatures: Implications for ozone chemistry in the polar marine boundary layer, *Journal of Geophysical Research: Atmospheres*, 105, 26393-26402, 10.1029/2000jd900413, 2000.
- 495 Koop, T., Bookhold, J., Shiraiwa, M., and Poschl, U.: Glass transition and phase state of organic compounds: dependency on molecular properties and implications for secondary organic aerosols in the atmosphere, *Physical Chemistry Chemical Physics*, 13, 19238-19255, 10.1039/c1cp22617g, 2011.
- 500 Laskin, A., Laskin, J., and Nizkorodov, S. A.: Chemistry of Atmospheric Brown Carbon, *Chemical Reviews*, 115, 4335-4382, 10.1021/cr5006167, 2015.
- Laskin, J., Laskin, A., Roach, P. J., Slysz, G. W., Anderson, G. A., Nizkorodov, S. A., Bones, D. L., and Nguyen, L. Q.: High-Resolution Desorption Electrospray Ionization Mass Spectrometry for Chemical Characterization of Organic Aerosols, *Analytical Chemistry*, 82, 2048-2058, 10.1021/ac902801f, 2010.
- 505 Lee, H. D., Ray, K. K., and Tivanski, A. V.: Solid, Semisolid, and Liquid Phase States of Individual Submicrometer Particles Directly Probed Using Atomic Force Microscopy, *Analytical Chemistry*, 89, 12720-12726, 10.1021/acs.analchem.7b02755, 2017.
- Lee, H. J., Laskin, A., Laskin, J., and Nizkorodov, S. A.: Excitation–Emission Spectra and Fluorescence Quantum Yields for Fresh and Aged Biogenic Secondary Organic Aerosols, *Environmental Science & Technology*, 47, 5763-5770, 10.1021/es400644c, 2013.
- 510 Li, Y. J., Liu, P., Gong, Z., Wang, Y., Bateman, A. P., Bergoend, C., Bertram, A. K., and Martin, S. T.: Chemical Reactivity and Liquid/Nonliquid States of Secondary Organic Material, *Environmental Science & Technology*, 49, 13264-13274, 10.1021/acs.est.5b03392, 2015.
- Lignell, H., Hinks, M. L., and Nizkorodov, S. A.: Exploring matrix effects on photochemistry of organic aerosols, *Proceedings of the National Academy of Sciences*, 111, 13780-13785, 10.1073/pnas.1322106111, 2014.
- 515 Liu, P., Li, Y. J., Wang, Y., Gilles, M. K., Zaveri, R. A., Bertram, A. K., and Martin, S. T.: Lability of secondary organic particulate matter, *Proceedings of the National Academy of Sciences*, 113, 12643-12648, 10.1073/pnas.1603138113, 2016.
- Longinotti, M. P., and Corti, H. R.: Diffusion of ferrocene methanol in super-cooled aqueous solutions using cylindrical microelectrodes, *Electrochemistry Communications*, 9, 1444-1450, <http://dx.doi.org/10.1016/j.elecom.2007.02.003>, 2007.
- 520 Maclean, A. M., Butenhoff, C. L., Grayson, J. W., Barsanti, K., Jimenez, J. L., and Bertram, A. K.: Mixing times of organic molecules within secondary organic aerosol particles: a global planetary boundary layer perspective, *Atmos. Chem. Phys.*, 17, 13037-13048, 10.5194/acp-17-13037-2017, 2017.
- Marsh, A., Rovelli, G., Song, Y.-C., Pereira, K. L., Willoughby, R. E., Bzdek, B. R., Hamilton, J. F., Orr-Ewing, A. J., Topping, D. O., and Reid, J. P.: Accurate representations of the physicochemical properties of atmospheric aerosols: when are laboratory measurements of value?, *Faraday Discussions*, 200, 639-661, 2017.
- 525 Massoli, P., Lambe, A. T., Ahern, A. T., Williams, L. R., Ehn, M., Mikkilä, J., Canagaratna, M. R., Brune, W. H., Onasch, T. B., Jayne, J. T., Petäjä, T., Kulmala, M., Laaksonen, A., Kolb, C. E., Davidovits, P., and Worsnop, D. R.: Relationship between aerosol oxidation level and hygroscopic properties of laboratory generated secondary organic aerosol (SOA) particles, *Geophysical Research Letters*, 37, n/a-n/a, 10.1029/2010gl045258, 2010.
- 530 Meyvis, T. L., De Smedt, S., Van Oostveldt, P., and Demeester, J.: Fluorescence Recovery After Photobleaching: A Versatile Tool for Mobility and Interaction Measurements in Pharmaceutical Research, *Pharm Res*, 16, 1153-1162, 10.1023/a:1011924909138, 1999.
- Mikhailov, E., Vlasenko, S., Martin, S., Koop, T., and Pöschl, U.: Amorphous and crystalline aerosol particles interacting with water vapor: conceptual framework and experimental evidence for restructuring, phase transitions and kinetic limitations, *Atmospheric Chemistry and Physics*, 9, 9491-9522, 2009.
- 535 Murray, B. J., Wilson, T. W., Dobbie, S., Cui, Z., Al-Jumur, S. M. R. K., Mohler, O., Schnaiter, M., Wagner, R., Benz, S., Niemand, M., Saathoff, H., Ebert, V., Wagner, S., and Karcher, B.: Heterogeneous nucleation of ice particles on glassy aerosols under cirrus conditions, *Nature Geosci*, 3, 233-237, 10.1038/ngeo817, 2010.

- Nguyen, T. B., Laskin, A., Laskin, J., and Nizkorodov, S. A.: Brown carbon formation from ketoaldehydes of biogenic monoterpenes, *Faraday Discussions*, 165, 473-494, 10.1039/c3fd00036b, 2013.
- Nozière, B., Kalberer, M., Claeys, M., Allan, J., D'Anna, B., Decesari, S., Finessi, E., Glasius, M., Grgić, I., Hamilton, J. F., Hoffmann, T., Inuma, Y., Jaoui, M., Kahnt, A., Kampf, C. J., Kourtev, I., Maenhaut, W., Marsden, N., Saarikoski, S., Schnelle-Kreis, J., Surratt, J. D., Szidat, S., Szmigielski, R., and Wisthaler, A.: The Molecular Identification of Organic Compounds in the Atmosphere: State of the Art and Challenges, *Chemical Reviews*, 115, 3919-3983, 10.1021/cr5003485, 2015.
- Perraud, V., Bruns, E. A., Ezell, M. J., Johnson, S. N., Yu, Y., Alexander, M. L., Zelenyuk, A., Imre, D., Chang, W. L., Dabdub, D., Pankow, J. F., and Finlayson-Pitts, B. J.: Nonequilibrium atmospheric secondary organic aerosol formation and growth, *Proceedings of the National Academy of Sciences*, 109, 2836-2841, 10.1073/pnas.1119909109, 2012.
- Poschl, U., and Shiraiwa, M.: Multiphase Chemistry at the Atmosphere-Biosphere Interface Influencing Climate and Public Health in the Anthropocene, *Chemical Reviews*, 115, 4440-4475, 10.1021/cr500487s, 2015.
- Power, R. M., Simpson, S. H., Reid, J. P., and Hudson, A. J.: The transition from liquid to solid-like behaviour in ultrahigh viscosity aerosol particles, *Chemical Science*, 4, 2597-2604, 10.1039/c3sc50682g, 2013.
- Price, H. C., Mattsson, J., Zhang, Y., Bertram, A. K., Davies, J. F., Grayson, J. W., Martin, S. T., O'Sullivan, D., Reid, J. P., and Rickards, A. M.: Water diffusion in atmospherically relevant  $\alpha$ -pinene secondary organic material, *Chemical Science*, 6, 4876-4883, 2015.
- Price, H. C., Mattsson, J., and Murray, B. J.: Sucrose diffusion in aqueous solution, *Physical Chemistry Chemical Physics*, 18, 19207-19216, 10.1039/C6CP03238A, 2016.
- Pye, H. O. T., Chan, A. W. H., Barkley, M. P., and Seinfeld, J. H.: Global modeling of organic aerosol: the importance of reactive nitrogen ( $\text{NO}_x$  and  $\text{NO}_3$ ), *Atmos. Chem. Phys.*, 10, 11261-11276, 10.5194/acp-10-11261-2010, 2010.
- Reid, J. P., Bertram, A. K., Topping, D. O., Laskin, A., Martin, S. T., Petters, M. D., Pope, F. D., and Rovelli, G.: The viscosity of atmospherically relevant organic particles, *Nature Communications*, 9, 956, 10.1038/s41467-018-03027-z, 2018.
- Renbaum-Wolff, L., Grayson, J. W., Bateman, A. P., Kuwata, M., Sellier, M., Murray, B. J., Shilling, J. E., Martin, S. T., and Bertram, A. K.: Viscosity of  $\alpha$ -pinene secondary organic material and implications for particle growth and reactivity, *Proceedings of the National Academy of Sciences*, 110, 8014-8019, 10.1073/pnas.1219548110, 2013a.
- Renbaum-Wolff, L., Grayson, J. W., and Bertram, A. K.: Technical Note: New methodology for measuring viscosities in small volumes characteristic of environmental chamber particle samples, *Atmos. Chem. Phys.*, 13, 791-802, 10.5194/acp-13-791-2013, 2013b.
- Riipinen, I., Pierce, J., Yli-Juuti, T., Nieminen, T., Hakkinen, S., Ehn, M., Junninen, H., Lehtipalo, K., Petaja, T., and Slowik, J.: Organic condensation: a vital link connecting aerosol formation to cloud condensation nuclei (CCN) concentrations, *Atmospheric Chemistry and Physics*, 11, 3865, 10.5194/acp-11-3865-2011, 2011.
- Robinson, C. B., Schill, G. P., and Tolbert, M. A.: Optical growth of highly viscous organic/sulfate particles, *Journal of Atmospheric Chemistry*, 71, 145-156, 10.1007/s10874-014-9287-8, 2014.
- Saathoff, H., Naumann, K. H., Möhler, O., Jonsson, Å. M., Hallquist, M., Kiendler-Scharr, A., Mentel, T. F., Tillmann, R., and Schurath, U.: Temperature dependence of yields of secondary organic aerosols from the ozonolysis of  $\alpha$ -pinene and limonene, *Atmos. Chem. Phys.*, 9, 1551-1577, 10.5194/acp-9-1551-2009, 2009.
- Schneider, C. A., Rasband, W. S., and Eliceiri, K. W.: NIH Image to ImageJ: 25 years of image analysis, *Nat methods*, 9, 671-675, 2012.
- Seinfeld, J. H., and Pandis, S. N.: *Atmospheric chemistry and physics: from air pollution to climate change*, John Wiley & Sons, 2016.
- Seksek, O., Biwersi, J., and Verkman, A. S.: Translational Diffusion of Macromolecule-sized Solutes in Cytoplasm and Nucleus, *The Journal of Cell Biology*, 138, 131-142, 10.1083/jcb.138.1.131, 1997.
- Shiraiwa, M., Ammann, M., Koop, T., and Pöschl, U.: Gas uptake and chemical aging of semisolid organic aerosol particles, *Proceedings of the National Academy of Sciences*, 108, 11003-11008, 10.1073/pnas.1103045108, 2011.
- Shiraiwa, M., and Seinfeld, J. H.: Equilibration timescale of atmospheric secondary organic aerosol partitioning, *Geophysical Research Letters*, 39, n/a-n/a, 10.1029/2012gl054008, 2012.
- Shiraiwa, M., Zuend, A., Bertram, A. K., and Seinfeld, J. H.: Gas-particle partitioning of atmospheric aerosols: interplay of physical state, non-ideal mixing and morphology, *Physical Chemistry Chemical Physics*, 15, 11441-11453, 2013.

- Shiraiwa, M., Li, Y., Tsimpidi, A. P., Karydis, V. A., Berkemeier, T., Pandis, S. N., Lelieveld, J., Koop, T., and Pöschl, U.: Global distribution of particle phase state in atmospheric secondary organic aerosols, *Nature Communications*, 8, 15002, 10.1038/ncomms15002  
590 <https://www.nature.com/articles/ncomms15002#supplementary-information>, 2017a.
- Shiraiwa, M., Ueda, K., Pozzer, A., Lammel, G., Kampf, C. J., Fushimi, A., Enami, S., Arangio, A. M., Frohlich-Nowoisky, J., Fujitani, Y., Furuyama, A., Lakey, P. S. J., Lelieveld, J., Lucas, K., Morino, Y., Poschl, U., Takaharna, S., Takami, A., Tong, H. J., Weber, B., Yoshino, A., and Sato, K.: Aerosol Health Effects from Molecular to Global Scales, *Environmental Science & Technology*, 51, 13545-13567, 10.1021/acs.est.7b04417, 2017b.  
595
- Shrivastava, M., Cappa, C. D., Fan, J., Goldstein, A. H., Guenther, A. B., Jimenez, J. L., Kuang, C., Laskin, A., Martin, S. T., Ng, N. L., Petaja, T., Pierce, J. R., Rasch, P. J., Roldin, P., Seinfeld, J. H., Shilling, J., Smith, J. N., Thornton, J. A., Volkamer, R., Wang, J., Worsnop, D. R., Zaveri, R. A., Zelenyuk, A., and Zhang, Q.: Recent advances in understanding secondary organic aerosol: Implications for global climate forcing, *Reviews of Geophysics*, 55, 509-559, 10.1002/2016rg000540, 2017a.
- Shrivastava, M., Lou, S., Zelenyuk, A., Easter, R. C., Corley, R. A., Thrall, B. D., Rasch, P. J., Fast, J. D., Massey Simonich, S. L., Shen, H., and Tao, S.: Global long-range transport and lung cancer risk from polycyclic aromatic hydrocarbons shielded by coatings of organic aerosol, *Proceedings of the National Academy of Sciences*, 114, 1246-1251, 10.1073/pnas.1618475114, 2017b.  
600
- Sindelarova, K., Granier, C., Bouarar, I., Guenther, A., Tilmes, S., Stavrakou, T., Muller, J. F., Kuhn, U., Stefani, P., and Knorr, W.: Global data set of biogenic VOC emissions calculated by the MEGAN model over the last 30 years, *Atmospheric Chemistry and Physics*, 14, 9317-9341, 10.5194/acp-14-9317-2014, 2014.  
605
- Sinnecker, D., Voigt, P., Hellwig, N., and Schaefer, M.: Reversible Photobleaching of Enhanced Green Fluorescent Proteins, *Biochemistry*, 44, 7085-7094, 10.1021/bi047881x, 2005.
- Solomon, S.: Climate change 2007-the physical science basis: Working group I contribution to the fourth assessment report of the IPCC, Cambridge University Press, 2007.  
610
- Solomon, S., D. Qin, M. Manning, Z. Chen, M. Marquis, K.B. Averyt, M. Tignor and, and (eds.), H. L. M.: IPCC Fourth Assessment Report: Climate Change 2007: The Physical Science Basis: Contribution of Working Group I to the Fourth Assessment Report of the Intergovernmental Panel on Climate Change, Cambridge University Press, Cambridge, United Kingdom and New York, NY, USA, 996 pp., 2007.
- Song, M., Liu, P. F., Hanna, S. J., Li, Y. J., Martin, S. T., and Bertram, A. K.: Relative humidity-dependent viscosities of isoprene-derived secondary organic material and atmospheric implications for isoprene-dominant forests, *Atmos. Chem. Phys.*, 15, 5145-5159, 10.5194/acp-15-5145-2015, 2015.  
615
- Song, M., Liu, P. F., Hanna, S. J., Zaveri, R. A., Potter, K., You, Y., Martin, S. T., and Bertram, A. K.: Relative humidity-dependent viscosity of secondary organic material from toluene photo-oxidation and possible implications for organic particulate matter over megacities, *Atmospheric Chemistry and Physics*, 16, 8817-8830, 10.5194/acp-16-8817-2016, 2016.  
620
- Spracklen, D. V., Jimenez, J. L., Carslaw, K. S., Worsnop, D. R., Evans, M. J., Mann, G. W., Zhang, Q., Canagaratna, M. R., Allan, J., Coe, H., McFiggans, G., Rap, A., and Forster, P.: Aerosol mass spectrometer constraint on the global secondary organic aerosol budget, *Atmos. Chem. Phys.*, 11, 12109-12136, 10.5194/acp-11-12109-2011, 2011.
- Stout, A. L., and Axelrod, D.: SPONTANEOUS RECOVERY OF FLUORESCENCE BY PHOTOBLEACHED SURFACE-ADSORBED PROTEINS, *Photochemistry and Photobiology*, 62, 239-244, 10.1111/j.1751-1097.1995.tb05264.x, 1995.  
625
- Taina, Y. J., Aki, P., Olli-Pekka, T., Angela, B., Celia, F., Olli, V., Liqing, H., Eetu, K., Otso, P., Olga, G., Manabu, S., Mikael, E., Kari, L., and Annele, V.: Factors controlling the evaporation of secondary organic aerosol from  $\alpha$ -pinene ozonolysis, *Geophysical Research Letters*, 44, 2562-2570, doi:10.1002/2016GL072364, 2017.
- Verkman, A. S.: [28] Diffusion in cells measured by fluorescence recovery after photobleaching, *Methods in Enzymology*, 360, 635-648, 10.1016/S0076-6879(03)60132-1, 2003.  
630
- Wagner, R., Höhler, K., Huang, W., Kiselev, A., Möhler, O., Mohr, C., Pajunoja, A., Saathoff, H., Schiebel, T., and Shen, X.: Heterogeneous ice nucleation of  $\alpha$ -pinene SOA particles before and after ice cloud processing, *Journal of Geophysical Research: Atmospheres*, 122, 4924-4943, 2017.
- Wang, B., Lambe, A. T., Massoli, P., Onasch, T. B., Davidovits, P., Worsnop, D. R., and Knopf, D. A.: The deposition ice nucleation and immersion freezing potential of amorphous secondary organic aerosol: Pathways for ice and mixed-phase cloud formation, *Journal of Geophysical Research: Atmospheres*, 117, n/a-n/a, 10.1029/2012jd018063, 2012.  
635

- Wang, B., O'Brien, R. E., Kelly, S. T., Shilling, J. E., Moffet, R. C., Gilles, M. K., and Laskin, A.: Reactivity of Liquid and Semisolid Secondary Organic Carbon with Chloride and Nitrate in Atmospheric Aerosols, *The Journal of Physical Chemistry A*, 119, 4498-4508, 10.1021/jp510336q, 2015.
- 640 Ye, Q., Robinson, E. S., Ding, X., Ye, P., Sullivan, R. C., and Donahue, N. M.: Mixing of secondary organic aerosols versus relative humidity, *Proceedings of the National Academy of Sciences*, 113, 12649-12654, 10.1073/pnas.1604536113, 2016.
- Ye, Q., Upshur, M. A., Robinson, E. S., Geiger, F. M., Sullivan, R. C., Thomson, R. J., and Donahue, N. M.: Following Particle-Particle Mixing in Atmospheric Secondary Organic Aerosols by Using Isotopically Labeled Terpenes, *Chem*, 4, 318-333, 10.1016/j.chempr.2017.12.008, 2018.
- 645 Zaveri, R. A., Easter, R. C., Shilling, J. E., and Seinfeld, J. H.: Modeling kinetic partitioning of secondary organic aerosol and size distribution dynamics: representing effects of volatility, phase state, and particle-phase reaction, *Atmos. Chem. Phys.*, 14, 5153-5181, 10.5194/acp-14-5153-2014, 2014.
- Zaveri, R. A., Shilling, J. E., Zelenyuk, A., Liu, J., Bell, D. M., D'Ambro, E. L., Gaston, C. J., Thornton, J. A., Laskin, A., Lin, P., Wilson, J., Easter, R. C., Wang, J., Bertram, A. K., Martin, S. T., Seinfeld, J. H., and Worsnop, D. R.: Growth Kinetics and Size Distribution Dynamics of Viscous Secondary Organic Aerosol, *Environmental Science & Technology*, 52, 1191-1199, 10.1021/acs.est.7b04623, 2018.
- 650 Zelenyuk, A., Imre, D., Beránek, J., Abramson, E., Wilson, J., and Shrivastava, M.: Synergy between Secondary Organic Aerosols and Long-Range Transport of Polycyclic Aromatic Hydrocarbons, *Environmental Science & Technology*, 46, 12459-12466, 10.1021/es302743z, 2012.
- 655 Zhang, Y., Sanchez, M. S., Douet, C., Wang, Y., Bateman, A. P., Gong, Z., Kuwata, M., Renbaum-Wolff, L., Sato, B. B., Liu, P. F., Bertram, A. K., Geiger, F. M., and Martin, S. T.: Changing shapes and implied viscosities of suspended submicron particles, *Atmos. Chem. Phys.*, 15, 7819-7829, 10.5194/acp-15-7819-2015, 2015.
- Zhou, S., Lee, A. K. Y., McWhinney, R. D., and Abbatt, J. P. D.: Burial Effects of Organic Coatings on the Heterogeneous Reactivity of Particle-Borne Benzo[a]pyrene (BaP) toward Ozone, *The Journal of Physical Chemistry A*, 116, 7050-7056, 10.1021/jp3030705, 2012.
- 660 Zobrist, B., Soonsin, V., Luo, B. P., Krieger, U. K., Marcolli, C., Peter, T., and Koop, T.: Ultra-slow water diffusion in aqueous sucrose glasses, *Physical Chemistry Chemical Physics*, 13, 3514-3526, 10.1039/C0CP01273D, 2011.